Indirect Role of Ca^{2+} in the Assembly of Extracellular Matrix Proteins

Jiankuai Diao and Emad Tajkhorshid
Department of Biochemistry, Beckman Institute, and Center for Biophysics and Computational Biology, University of Illinois at Urbana-Champaign, Urbana, Illinois

ABSTRACT We have investigated through molecular dynamics the binding properties at the interface between the C-type lectin subdomain (CLD) of aggrecan and the fibronectin type III domains ($^{4-5}$FnIII) of tenasin, in particular the mechanistically unknown, but essential role of Ca^{2+} in the binding. The binding between the CLD and $^{4-5}$FnIII is critical in cross-linking aggrecan, hyaluronan, and tenascin to form extended protein networks found in tissues such as cartilage. None of the structurally resolved Ca^{2+} ions in the complex of the CLD and $^{4-5}$FnIII is directly bridging the two proteins. However, one of the Ca^{2+} ions (Ca2) is found to play the role of maintaining the structure of the L4 loop at the CLD binding surface, thus facilitating a high affinity binding between the CLD and $^{4-5}$FnIII. Removal of this Ca^{2+} ion causes a drastic structural change in the L4 loop, which presumably hinders the binding of the CLD to the $^{4-5}$FnIII. The other bound Ca^{2+} ions (Ca1 and Ca3) have no significant effect on the structure of the CLD binding surface, and thus are not expected to affect the binding. Our results might also suggest that the role of Ca2 in maintaining the structure of the L4 loop is most important during the binding process. Once the complex is formed, the dependence of the complex on the structuring role of Ca2 is reduced. In response to tensile force, the CLD and $^{4-5}$FnIII separate by breaking first the electrostatic interactions at the interface, followed by the hydrophobic ones. The sequence of the unbinding events and the maximum force required to separate the two proteins are independent of the presence of the Ca^{2+} ions, underlying the indirect role of Ca^{2+} in the binding.

INTRODUCTION

Extracellular matrix (ECM) proteins are multimodular and multifunctional molecules, whose components are produced intracellularly and secreted into the ECM. They assemble into well-organized protein networks in the ECM and provide structural and biomechanical properties crucial for survival, proliferation, and differentiation of cells. However, the mechanisms by which different ECM proteins assemble into complex yet well-organized networks are largely unknown, especially at the structural level. Atomic resolution structures of a number of ECM protein modules have been resolved using x-ray crystallography and NMR spectroscopy (1). These structures provide structural basis for certain functional aspects of the ECM proteins. The majority of the resolved structures, however, are those of individual protein modules or tandem modules of same proteins. Only recently, a few structures of complexes of different ECM proteins were resolved, enabling us to begin to understand at the atomic level the interactions involved in their assembly into ECM networks (1–3).

One of such complex structures is the x-ray structure of the C-type lectin subdomain (CLD) of aggrecan and the FnIII domains ($^{3-5}$FnIII) of tenasin resolved by Lundell et al. (2) (Fig. 1). The authors proposed that the interactions between the CLD and $^{3-5}$FnIII are responsible for cross-linking the aggrecan-hyaluronan complexes to form extended protein networks, which is supported by their electron microscopy study showing the cross-linked tenascin and aggrecan-hyaluronan molecules (2).

Aggrecan is the most extensively studied lectican. Lecticans have in common 1), an N-terminal globular G1 domain that binds hyaluronan via a linker protein; 2), a C-terminal globular G3 domain that binds to various proteins including tenascin; and 3), a central elongated domain with covalently linked glycosaminoglycan side chains (4). Aggrecan is responsible for generating a large osmotic swelling pressure in tissues such as cartilage, which is critical to the mechanical properties of these tissues. Negatively charged anionic groups on the glycosaminoglycan side chains of aggrecan attract and carry mobile counterions, e.g., Na^+, thus creating a large difference in ion concentration between the cartilage and the surrounding tissues. Consequently, water is drawn into the cartilage, causing the aggrecan matrix network to swell and expand (4).

Tenascins are expressed in the central nervous system and connective tissues during development, and reexpressed during wound healing. They bind to a variety of other components of the ECM, e.g., fibronectins and lecticans, and to cell surface receptors, such as integrin and cell adhesion molecules of the immunoglobulin superfamily. Tenascins are involved in a wide range of physiological processes, such as embryonic development and tissue remodeling (5). They all have a tenascin assembly domain at the N-terminus, followed by epidermal growth factorlike repeats, fibronectin type III (FnIII) repeats, and a C-terminal fibrinogenlike globular domain.

The interaction between aggrecan and tenascin is reported to be highly Ca^{2+}-dependent (6,7). However, in the complex

Submitted January 9, 2008, and accepted for publication February 29, 2008.

Address reprint requests to Emad Tajkhorshid, Tel.: 217-244-6914; E-mail: emad@life.uiuc.edu.

Editor: Peter Tieleman.

0006-3495/08/07/120/08 $2.00

doi: 10.1529/biophysj.108.129106

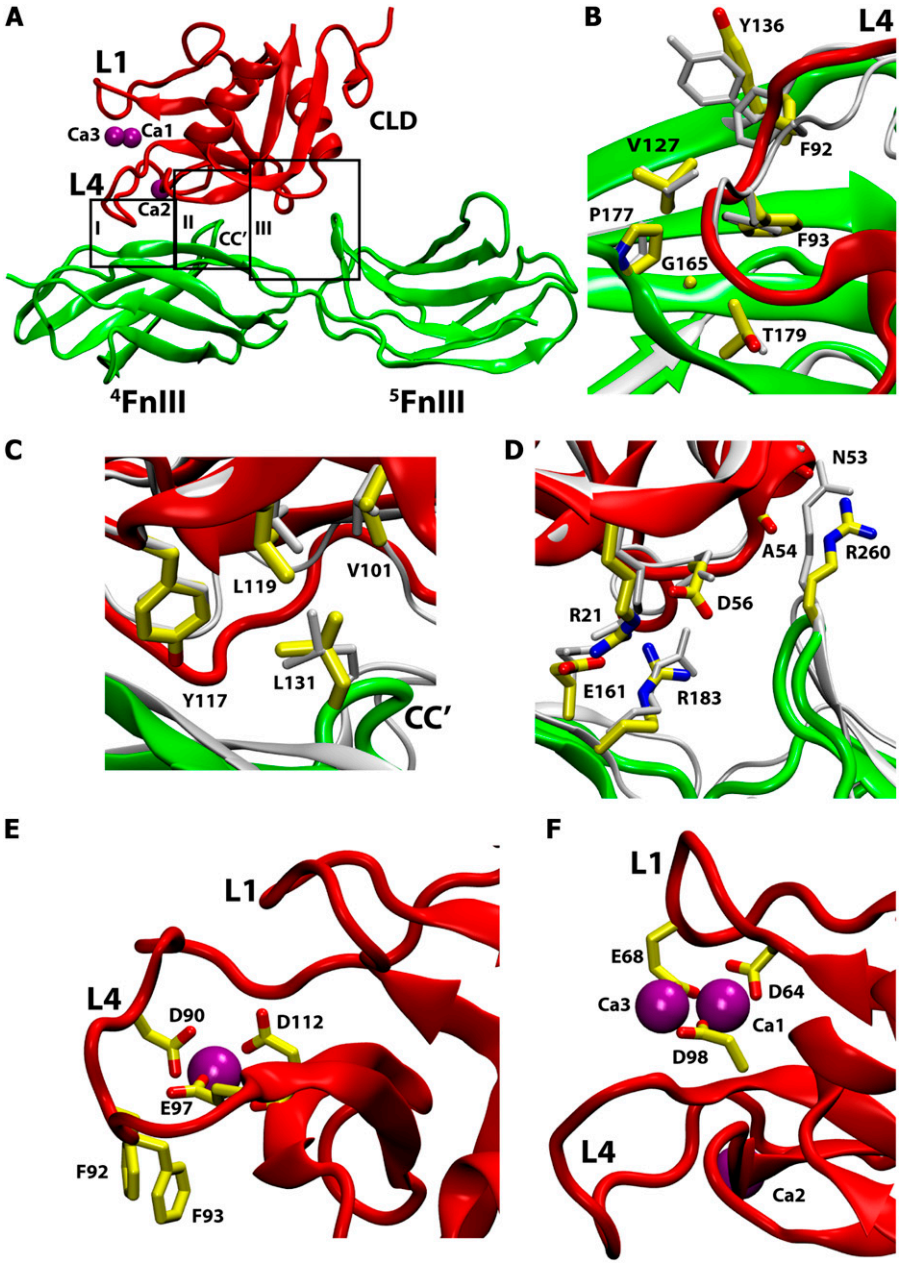

FIGURE 1 Binding interface of the CLD and $^{4–5}$FnIII. The structures shown correspond to the last frame of the 10-ns equilibration of the complex with all the Ca^{2+} ions present (Sim1), with the crystallographic structures also shown in gray for comparison. The CLD is shown in red, and $^{4–5}$FnIII in green. (*A*) The binding interface is composed of three distinct binding/contact areas: two hydrophobic (*I* and *II*) and one electrostatic (*III*) binding areas. Details of interactions in these areas are shown in panels *B–D*. (*B*) Binding area *I*. Hydrophobic residues Phe^{92} and Phe^{93} at the tip of the L4 loop of the CLD bind into a hydrophobic pocket in ^{4}FnIII. (*C*) Binding area *II*. Hydrophobic residue Leu^{131} at the tip of loop CC′ of ^{4}FnIII binds into a hydrophobic pocket in CLD. (*D*) Binding area *III*. Salt bridges and hydrogen bonds are the main types of interaction here. (*E*) Binding site of Ca2. This Ca^{2+} ion maintains the structure of the L4 loop by bridging its Asp^{90} to Glu^{97} and Asp^{112} on the core of the CLD. (*F*) Binding site of Ca1 and Ca3. These Ca^{2+} ions maintain the structure of the L1 loop by bridging its Glu^{68} and Asp^{64} to Asp^{98} on the core of the CLD.

structure all of the resolved Ca^{2+} ions are only in contact with the CLD, i.e., none of them is close enough to the binding interface to directly mediate the interaction between aggrecan and tenascin. This is in contrast to the orthodox Ca^{2+}-mediated binding of biological systems (see for example, (8–10)), where Ca^{2+} ions engage in direct contacts with both binding partners, thus stabilizing the complex.

In the crystal structure of the complex of the CLD and $^{3–5}$FnIII, three Ca^{2+} ions have been resolved, termed Ca1, Ca2, and Ca3, respectively (see Fig. 1). Ca2 is found in all structurally characterized CLDs (2,11,12), and Ca1 is found in the majority of them, but Ca3 is not, suggesting that its presence in the crystal structure might be due to the high Ca^{2+} concentration used in the experiments (2). It was, therefore, proposed that Ca2 might play a structural role in maintaining the structure of the CLD binding surface, while the presence of Ca3 might be adventitious (2). The structural role of Ca^{2+} ions has been shown in many proteins (13–19), where the structural integrity is critical to the biological function. One might wonder how such a structural role of Ca^{2+} contributes to the binding of aggrecan and tenascin.

In this article, we test through molecular dynamics (MD) simulations the hypothetical structural role of Ca^{2+} ions, and examine how it contributes to the binding of the CLD and $^{4–5}$FnIII. Due to the biomechanical role of the aggrecan network, we have also studied the response of the binding interface to tensile force. We find that the highly complementary binding surfaces of separated CLD and $^{4–5}$FnIII are

almost identical to those in the complex structure, indicating that no major structural changes occur upon binding. Although none of the structurally resolved Ca^{2+} ions is directly at the interface, removal of Ca2 causes significant structural changes at the binding surface of the CLD, which may reduce its binding ability. Removal of the other two Ca^{2+} ions (Ca1 and Ca3) results in smaller structural changes, but does not affect the binding interface. Thus, our study not only confirms an indirect role of Ca^{2+} ions in the binding, but also suggests different involvements of Ca2 and Ca1/Ca3 in the process. The role of Ca2 is to maintain the structure of CLD binding surface, which facilitates the binding of two highly complementary binding surfaces, while Ca1 and Ca3 do not seem to have an effect on the binding. In response to tensile force, aggrecan and tenascin separate by breaking first the electrostatic interactions, followed by the hydrophobic ones. The maximum force required to separate the two proteins corresponds to the disruption of the electrostatic interactions. The unbinding sequence and maximum force are independent of Ca^{2+} ions, underlying the indirect role of Ca^{2+} in the binding.

METHODS

Model building

The crystallographic structure of the complex of the CLD of aggrecan and $^{3-5}$FnIII of tenascin (PDB code 1TDQ) (2) was obtained from the protein data bank. The ^{3}FnIII domain of tenascin does not interact with the CLD and was thus excluded. The complex structure of $^{4-5}$FnIII and the CLD with all the three Ca^{2+} ions was solvated in a water box of $100 \times 100 \times 100$ Å^3. Periodic boundary conditions were used in all directions. The size of each water box in the following simulations is adjusted to ensure at least 20 Å of distance between the protein and its images in the periodic cells. To neutralize the system and to maintain a physiological ion concentration, Na^+ and Cl^- ions were added to the system at a concentration of 100 mM.

Simulation protocol

All the simulations were performed with NAMD (20), with a time step of 1 fs. The CHARMM27 parameter set (21) with TIP3P water (22) was used for the simulations. The particle-mesh Ewald method (23) was employed for the computation of long-range electrostatic forces, and a cutoff with a switching function starting at 10 Å and reaching zero at 12 Å was used for van der Waals interactions. The interaction between the Ca^{2+} ions and the rest of the system is described by the electrostatic and van der Waals interactions, as parameterized in the CHARMM27 force field (21), i.e., no bonds exist between the Ca^{2+} ions and their binding pockets. In all the simulations, the temperature was maintained at 310 K via the Langevin dynamics with a damping coefficient, γ, of 0.5 ps^{-1}. The pressure was maintained at 1 atm via the Langevin Nosé-Hoover method (24,25).

Simulation systems

A summary of all simulation systems is given in Tables 1 and 2. Six equilibrium simulations (Sim1-Sim6, Table 1) were performed. All the systems were initially minimized for 5000 steps and equilibrated for 0.5 ns with proteins constrained to their initial structures. The systems were then further minimized for 5000 steps and equilibrated for 10–30 ns without any constraints.

TABLE 1 Equilibrium simulations

Simulation	System	Simulation time (ns)	Ca^{2+} ions
Sim1	CLD, $^{4-5}$FnIII	10	Ca1, Ca2, Ca3
Sim2	CLD, $^{4-5}$FnIII	30	None
Sim3	CLD	10	Ca1, Ca2, Ca3
Sim4	$^{4-5}$FnIII	10	N/A
Sim5	CLD	30	Ca1, Ca3
Sim6	CLD	30	Ca2

In Sim1, the complex of the CLD and $^{4-5}$FnIII was equilibrated for 10 ns in the presence of the three structurally resolved Ca^{2+} ions (Ca1, Ca2, and Ca3). In Sim2, all Ca^{2+} ions were removed from the final structure of Sim1, and the system was equilibrated for 30 ns, to examine whether removal of the Ca^{2+} ions would affect the structure of the complex of the CLD and $^{4-5}$FnIII. In Sim3 and Sim4, individual CLD and $^{4-5}$FnIII molecules taken from the final structure of Sim1 were solvated in separate water boxes, and each equilibrated for 10 ns. These simulations were to identify any structural changes at the binding interface of the CLD and $^{4-5}$FnIII upon their separation, or equivalently, if structural changes should occur upon binding. In Sim5 and Sim6, the CLD taken from the equilibrated structure of Sim3 was equilibrated for 30 ns, either in the absence of Ca2 (Sim5), or in the absence of Ca1 and Ca3 (Sim6). These two simulations were to identify the role of the three Ca^{2+} ions in the structural stability of the CLD. To maintain the neutrality of the system, whenever a Ca^{2+} ion was removed, two Na^+ ions were added to the system at random positions in bulk water.

We have also performed six pulling simulations (Pull1-Pull6, Table 2) to study how the complex of the CLD and $^{4-5}$FnIII, particularly their binding interface, is affected by tensile force in the ECM. The equilibrated structures of the complex taken from Sim1 (with all the Ca^{2+} ions present) and Sim2 (no Ca^{2+}) were chosen as the starting points for these simulations. In all the simulations, the two termini of $^{4-5}$FnIII were fixed and the CLD was pulled either from the N-terminus (Pull1-Pull4), or from the center of mass of the CLD (Pull5 and Pull6). Specifically, the N-terminal C_α atom or the center of mass of the CLD was subject to a harmonic constraint with a force constant of 486 pN/Å (7 kCal/(mol.Å^2)), that moved along the direction perpendicular to the binding interface at a constant velocity until the CLD and $^{4-5}$FnIII separated. The applied pulling velocity was 5 Å/ns in Pull1 and Pull2, and 1 Å/ns in Pull3-Pull6 (Table 2).

RESULTS AND DISCUSSION

The binding interface between the CLD and $^{4-5}$FnIII can be characterized as three main areas (2). These areas, denoted as *I*, *II*, and *III*, are shown in Fig. 1, for a snapshot taken after 10 ns of equilibration of the complex of the CLD and $^{4-5}$FnIII with all the three resolved Ca^{2+} ions present (Sim1). The three binding areas in the original crystallographic structure

TABLE 2 Pulling simulations performed on the complex of the CLD and $^{4-5}$FnIII

Simulation	Pulling speed (Å/ns)	Ca^{2+} ions	Pulled point	Simulation time (ns)
Pull1	5	Ca1, Ca2, Ca3	CLD N-terminus	9
Pull2	5	None	CLD N-terminus	9
Pull3	1	Ca1, Ca2, Ca3	CLD N-terminus	40
Pull4	1	None	CLD N-terminus	40
Pull5	1	Ca1, Ca2, Ca3	CLD center of mass	40
Pull6	1	None	CLD center of mass	40

are also shown for comparison, indicating that no major structural changes occur during the MD relaxation of the crystal structure. In binding area *I* (Fig. 1 *B*), hydrophobic residues Phe^{92} and Phe^{93} at the tip of the L4 loop of the CLD bind into a hydrophobic pocket in ^{4}FnIII formed by Tyr^{136}, VaL^{127}, $Gly^{165,}$ Pro^{177}, and Thr^{179}; in binding area *II* (Fig. 1 *C*), hydrophobic residue Leu^{131} at the tip of the CC' loop of ^{4}FnIII binds into a hydrophobic pocket in the CLD formed by Leu^{119}, Val^{101}, and Tyr^{117}; and in binding area *III* (Fig. 1 *C*), salt bridges between Glu^{161} on ^{4}FnIII and Arg^{21} on the CLD, and between Arg^{183} on ^{4}FnIII and Asp^{56} on the CLD, as well as the hydrogen bonds between Arg^{260} on ^{5}FnIII and the carbonyl groups of Asn^{53} and Ala^{54} stabilize the structure of the complex.

Indirect role of Ca^{2+} in the binding of the CLD and $^{4-5}$FnIII

The first two equilibrium simulations (Sim1 and Sim2) investigate the effect of the Ca^{2+} ions on the structure and dynamics of the complex of the CLD and $^{4-5}$FnIII. No major structural changes in the individual CLD and $^{4-5}$FnIII domains and at their binding interface are observed during the 10-ns equilibration of their complex in the presence of all the three Ca^{2+} ions; the backbone RMSDs of the CLD, $^{4-5}$FnIII, and of the complex level off to values of 1.5 Å, 2.3 Å, and 2.0 Å, respectively. During the 30-ns equilibration of the complex structure after removal of all Ca^{2+} ions (Sim2), small changes in the L1 and L4 loops (Fig. 2 *A*) of the CLD are observed. However, the magnitude of these changes is small. The backbone RMSDs of the CLD, $^{4-5}$FnIII, and the complex, plateau to 1.7 Å, 2.3 Å, and 2.2 Å, respectively. The small change at the L4 loop in the absence of the Ca^{2+} ions does not seem to weaken the binding in binding area *I*. For example, the van der Waals interaction energy of Phe^{92} and Phe^{93} in the CLD with all the hydrophobic residues in $^{4-5}$FnIII are comparable in the presence and absence of the three Ca^{2+} ions (9.6 ± 1.9 vs. 13.5 ± 2.0 kcal/mol). These results support the structural stability of the complex, but do not shed light on the role of Ca^{2+} ions in the binding. In fact, they might even argue against a role of Ca^{2+} in the binding, as the structure of the complex does not seem to be affected by the removal of the Ca^{2+} ions.

In the equilibrium simulations of individual CLD (in the presence of Ca^{2+} ions) and $^{4-5}$FnIII (Sim-3 and Sim-4), no structural changes are observed except a small change at the tip of L4 loop; their backbone RMSDs level off to values of 1.5 Å and 2.5 Å, respectively. Particularly, the approximately flat binding surface of the CLD, which includes the L4 loop, remains structurally invariant from that in the complex (Fig. 2 *B*). Only at the tip of the L4 loop, a small structural change is observed, which is caused by the separation of Phe^{92} and Phe^{93} from the hydrophobic pocket in $^{4-5}$FnIII where they used to be bound in the complex. As discussed later, this structural change is much smaller compared to that

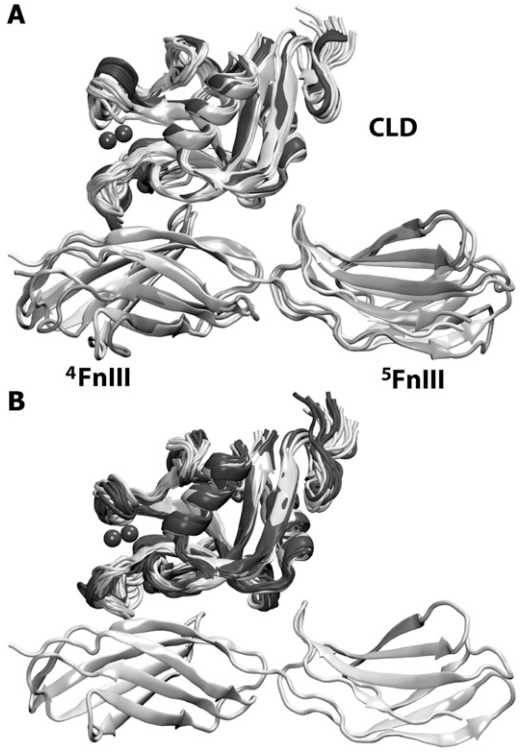

FIGURE 2 (*A*) Effect of Ca^{2+} ions to the structure of the complex. Ten frames of the CLD taken from the 10-ns equilibrium simulation of the complex in the absence of all the Ca^{2+} ions (Sim2) are shown in darker shading, and 10 frames of the CLD from the 10-ns simulation of the complex structure in the presence of the Ca^{2+} ions (Sim1) are shown in lighter shading. The time elapse between consecutive frames is 1 ns. Typical conformations of the $^{4-5}$FnIII in the absence (*darker shading*) and presence (*lighter shading*) of all the Ca^{2+} ions are also shown. The Ca^{2+} ions do not seem to have any significant effect on the structure of the complex. (*B*) Effect of binding on the structure of the binding surface of the CLD. Ten frames of the CLD taken from the 10-ns equilibrium simulation of isolated CLD (Sim3) are shown in darker shading, and 10 frames of the CLD from the 10-ns simulation of the complex structure (Sim1) in lighter shading. The time elapse between consecutive frames is 1 ns. The average structure of $^{4-5}$FnIII from the 10-ns equilibrium simulation of the complex is also shown. The structure of the CLD binding surface does not seem to be significantly affected by unbinding/binding to $^{4-5}$FnIII.

resulted from the removal of Ca2 from the isolated CLD (Sim5). The backbone RMSD of the L4 loop also levels off to 1.5 Å. The similarity of the structures of the individual CLD and $^{4-5}$FnIII modules to those in the complex suggests that no major structural changes accompany the binding of the two proteins, i.e., residues constituting the binding surfaces of the two proteins are already in the optimal position for the binding.

Removal of Ca2 significantly affects the structure of the CLD binding surface. Fig. 3 *A* compares the structures of the CLD in the presence and absence of Ca2 (Sim3 and Sim5, respectively). In the absence of Ca2, the L4 loop deviates significantly from that in the presence of Ca2. Therefore, Ca2 seems to be required for maintaining the structure of the L4 loop, which constitutes an important part of the CLD binding

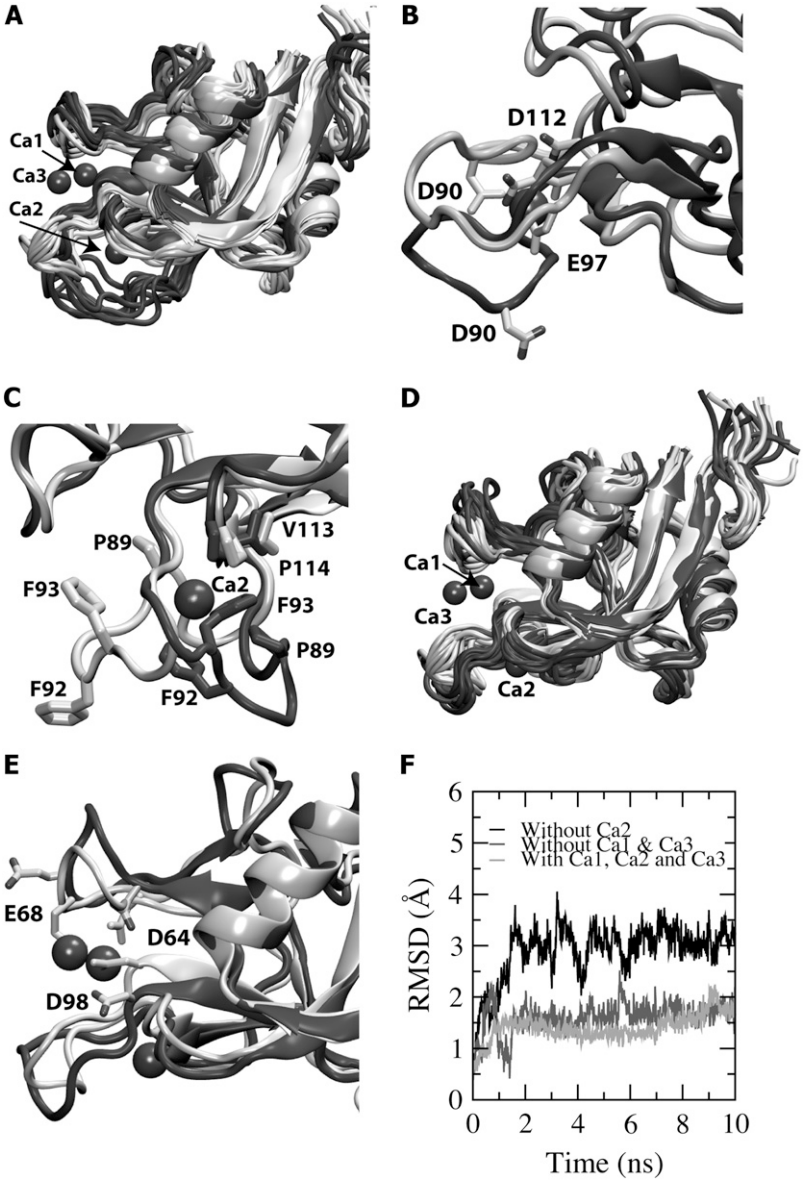

FIGURE 3 Structural role of Ca^{2+}. (*A*) Ten frames of conformations of the CLD in the presence (*lighter shading*) and absence (*darker shading*) of Ca2 taken from Sim3 and Sim5, respectively. (*B*) Representative configurations of the residues that coordinate Ca2 in the equilibration of the CLD in the presence (*lighter shading*) and absence of Ca2 (*darker shading*) taken from Sim3 and Sim5, respectively. (*C*) Representative configurations of the hydrophobic residues on the L4 loop in the equilibration of the CLD in the presence (*lighter shading*) and absence of Ca2 (*darker shading*) taken from Sim3 and Sim5, respectively. (*D*) An overlay of 10 frames of the CLD in the presence (*lighter shading*) and absence (*darker shading*) of Ca1 and Ca3, taken from Sim3 and Sim6, respectively. (*E*) Representative configurations of the residues that coordinate Ca1 and Ca3 in the equilibration of the CLD in the presence (*lighter shading*) and absence (*darker shading*) of Ca1 and Ca3 taken from Sim3 and Sim6, respectively. Shown in panel *F* are backbone RMSDs of the L4 loop in the absence of Ca2 (Sim5) and in the absence of Ca1 and Ca3 (Sim6), as well as that in the presence of all the Ca^{2+} ions (Sim3). The time elapse between consecutive frames in panels *A* and *D* is 1 ns.

surface. This structural role of Ca2 can be explained by the interactions depicted in Fig. 1 *E*; Ca2 maintains the structure of the L4 loop by bridging Asp^{90} on the L4 loop to Glu^{97} and Asp^{112} on the core of the CLD. Note also that Phe^{92} and Phe^{93}, which are responsible for hydrophobic interactions in binding area *I*, are situated between the residues Asp^{90} and Glu^{97} that coordinate Ca2 (Fig. 1 *E*). Thus, through maintaining the structure of the L4 loop, Ca2 not only preserves the flat structure of the CLD at the binding interface, but also keeps the critical binding residues, Phe^{92} and Phe^{93}, of the loop in optimal positions for binding. In the absence of Ca2, the negatively charged residues that coordinate Ca2 repel each other (Fig. 3 *B*), causing structural changes of the L4 loop (Fig. 3 *A*), which in turn result in repositioning of Phe^{92} and Phe^{93}. These effects altogether result in the destruction of the binding surface of the CLD.

In addition to Phe^{92} and Phe^{93}, there are other hydrophobic residues (Pro^{89} and Ala^{94}) on the L4 loop. In the presence of Ca2, all these hydrophobic residues are restrained in their positions and extend out into the solution (a representative configuration of which is shown in Fig. 3 *C*). After removal of Ca2, hydrophobic residues of the L4 loop gain a significantly higher flexibility and tend to cluster with themselves and with other hydrophobic residues, e.g., Pro^{114} and Val^{113} on the core structure of the CLD. A representative configuration of these residues during the 30-ns equilibration in the absence of Ca2 is also shown in Fig. 3 *C*. The clustering of these hydrophobic residues constitutes another driving force for the conformational change of the L4 loop (Fig. 3 *C*).

In contrast to Ca2, Ca1 and Ca3 do not seem to affect the binding surface. Fig. 3 *D* shows the conformations of the CLD in the presence and absence of these two ions (Sim3 and

Sim6, respectively). A much smaller structural change is observed at the CLD binding surface when Ca1 and Ca3 are removed, in comparison to the removal of Ca2. This can be explained by interactions depicted in Fig. 1 *F*: Ca1 and Ca3 maintain the structure of the L1 loop, not the L4 loop, by bridging Glu^{68} and Asp^{64} on the L1 loop to Asp^{98} on the core of the CLD. The removal of Ca1 and Ca3 also causes the carboxylate ligands (Asp^{64}, Glu^{68}, and Asp^{98}) to repel each other, and affect the structure of the L1 loop (Fig. 3 *E*). Due to the proximity of Asp^{98} to the L4 loop (Fig. 1 *F*), the removal of Ca1 and Ca3 also has some effect on the L4 loop, but this effect is much smaller compared to the removal of Ca2. Overall, the main effect of the removal of Ca1 and Ca3 is an increase of the distance between the L1 and L4 loops (Fig. 1 *D*).

Fig. 3 *F* compares the RMSDs of the L4 loop after removal of Ca2 and after removal of Ca1 and Ca3 (Sim5 and Sim6). A much larger RMSD is observed when Ca2 is removed compared to when Ca1 and Ca3 are removed. Also note that the RMSDs are comparable when Ca1 and Ca3 are removed and when all the Ca^{2+} ions are present. Altogether, our results do not support a role for Ca1 and Ca3 in the binding of CLD and $^{4-5}$FnIII.

Tension-induced unbinding of the CLD and $^{4-5}$FnIII

We next looked at the response of the binding interface to external forces and investigated the effect of the Ca^{2+} ions on the sequence of unbinding events and the force required for unbinding of the CLD and $^{4-5}$FnIII. In the first four of these simulations, the CLD was pulled from its N-terminus along the direction perpendicular to the binding interface (Fig. 4) at different pulling speeds (5 Å/ns and 1 Å/ns), and in the absence or the presence of the Ca^{2+} ions (Table 2). The tensile loading results in the unbinding of the CLD from $^{4-5}$FnIII by breaking first the electrostatic interactions (binding area *III* in Fig. 1), both in the presence and the absence of the Ca^{2+} ions, at both pulling speeds (Fig. 4). Once the electrostatic interactions are broken, the hydrophobic interactions in binding areas *I* and *II* break rapidly. The sequence of unbinding events does not appear to depend on Ca^{2+} ions. The force profiles are also similar in the presence and the absence of the Ca^{2+} ions; the maximum forces correspond to breaking of the electrostatic interactions in binding area *III* (Fig. 4), and are independent of the Ca^{2+} ions, which reside in binding area *I* (Fig. 4).

To ensure that the sequence of the unbinding events is also independent of the pulling protocol, in the last two pulling simulations (Pull5 and Pull6), the CLD was pulled from its center of mass at a speed of 1 Å/ns. These simulations resulted in the same sequence of unbinding events; the electrostatic interactions in binding area *III* break first, and then the hydrophobic interactions in binding areas *I* and *II*. Force profiles are also similar, in the sense that the maximum forces always correspond to the disruption of the electrostatic interactions in binding area *III*. Independence of the forces and the unbinding sequence on the Ca^{2+} ions further underlines the indirect role of Ca^{2+} ions in the binding process.

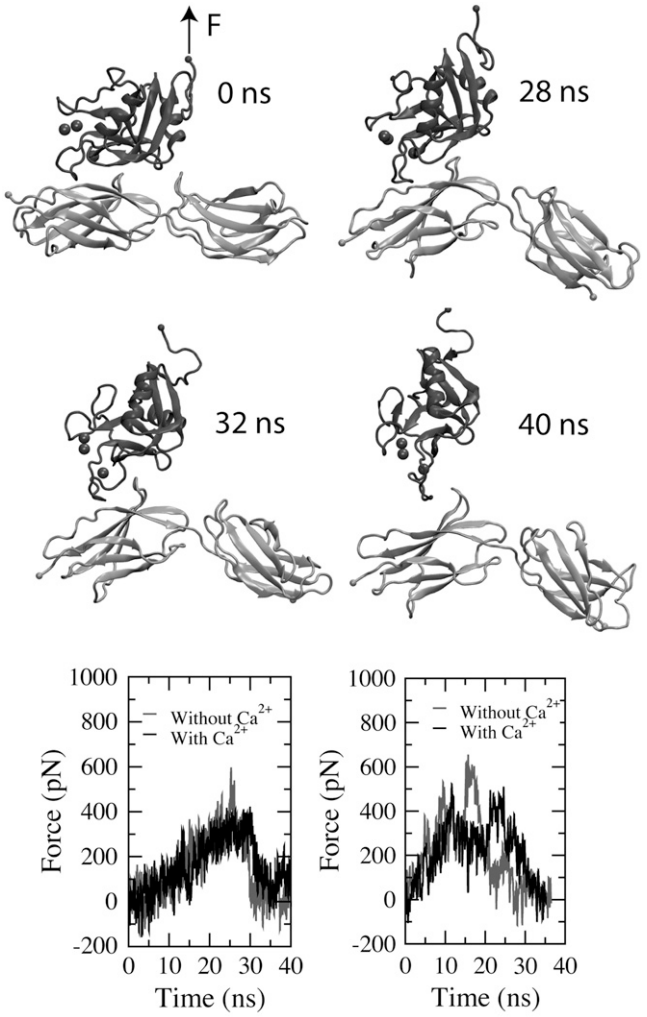

FIGURE 4 Unbinding of the CLD and $^{4-5}$FnIII. The snapshots shown are taken from the simulation in the presence of all the Ca^{2+} ions (Pull3), with the CLD pulled from its N-terminus. The forces during the pulling are also shown as a function of time (*left panel*: Pull3 and Pull4, pulled from the N-terminus; *right panel*: Pull5 and Pull6, pulled from the center of mass).

There are, however, minor differences in the detailed force profiles between these two pulling protocols. Two distinct peaks in the force profile are seen when the CLD is pulled from the center of mass in the presence of the Ca^{2+} ions. This is caused by a small difference in the breaking the electrostatic interactions in binding area *III*. In this simulation, the binding area *III* breaks in two steps by first breaking the hydrogen bonds formed between Arg^{260} on ^{5}FnIII and the carbonyl groups of Asn^{53} and Ala^{54} (Fig. 1 *C*), followed by the breaking of the salt bridges between Glu^{161} on ^{4}FnIII and Arg^{21} on the CLD, and between Arg^{183} on ^{4}FnIII and Asp^{56} on the CLD. In all the other pulling simulations, these hydrogen bonds and

salt bridges break approximately at the same time, and thus only one major peak is observed. This difference is likely due to the stochastic nature of the process, rather than the effect of the Ca^{2+} ions, since the ions are all localized around the binding area *I*, i.e., far away from the electrostatic interactions in the binding area *III*. Also, note that it takes a longer simulation time to induce unbinding when the CLD is pulled from the N-terminus. This is mainly due to the long floppy N-terminus, which extends during the initial phase of the pulling simulations, rather than any effect caused by the Ca^{2+} ions.

CONCLUSION

The extracellular matrix (ECM) is an extremely important component, both structurally and physiologically, in multicellular organisms. Through providing a scaffold, the ECM plays an important role in anchoring and motion of individual cells, thus affecting, e.g., tissue integrity and metastasis of cancer cells. Apart from its static, structural role, the dynamics of the ECM and its response to mechanical tension are also physiologically important, as they constitute key mechanisms for signal transduction between the cell and its environment. As such, mechanical properties of the ECM proteins have been extensively studied.

The ECM is composed of a large number of proteins, usually in tandem, that form an extensive, complex network through specific interactions. To understand the organization of the ECM and how it is affected by tensile force, which is constantly present in the ECM, it is necessary to understand the molecular details of interactions underlying the assembly of the ECM proteins. The binding of the CLD and $^{4-5}$FnIII, a highly Ca^{2+} dependent process, is one of the key interactions responsible for the assembly of aggrecan, hyaluronan, and tenascin into extended protein networks in the ECM.

In this study, we have used an extensive set of all-atom MD simulations to investigate the role of the Ca^{2+} ions in the binding of the CLD and $^{4-5}$FnIII, based on which we confirm an indirect role for Ca^{2+} in the binding of these proteins. None of the structurally bound Ca^{2+} ions provides a bridging role in the structure of the complex of the CLD and $^{4-5}$FnIII. Our simulations show, however, that one of the Ca^{2+} ions (Ca2) is crucial for structural stability of the binding interface, and that removal of this Ca^{2+} ion results in a significant destruction of the interface. Ca2 appears to play its role by anchoring the L4 loop to the core of the CLD, which in turn positions hydrophobic residues important for the binding (e.g., Phe^{92} and Phe^{93}) at their optimal binding conformations. The other two structurally resolved Ca^{2+} ions did not prove important for the binding.

In response to tensile force, the CLD and $^{4-5}$FnIII separate by breaking first their electrostatic interactions, and then the hydrophobic ones. The unbinding sequence and the force profiles are independent of the Ca^{2+} ions, an observation which further underlines the indirect role of Ca^{2+} in the binding.

Ca^{2+} ions play key structural roles in biological systems. They have been also implicated in the formation of complexes between different macromolecular structures where they usually directly and favorably interact with the two binding partners, thus stabilizing the complex. The system reported in this study is one of the first examples in which we demonstrate an indirect role for Ca^{2+} in the binding of two proteins. Along with the growing number of structurally resolved protein complexes, we might expect such an unusual role of Ca^{2+} to be a common mechanism in the assembly of multiprotein structures.

The authors acknowledge computer time on the ABE cluster at the National Center for Supercomputing Applications, the BigRed cluster at Indiana University (TERAGRID resources, grant No. MCA06N060), and the Turing cluster at the Computational Science and Engineering Program at the University of Illinois at Urbana-Champaign.

REFERENCES

1. Hohenester, E., and J. Engel. 2002. Domain structure and organization in extracellular matrix proteins. *Matrix Biol.* 21:115–128.
2. Lundell, A., A. I. Olin, M. Mörgelin, S. al-Karadaghi, A. Aspberg, and D. T. Logan. 2004. Structural basis for interactions between tenascins and lectican C-type lectin domains: evidence for a crosslinking role for tenascins. *Structure.* 12:1495–1506.
3. Takagi, J., Y. Yang, J. H. Liu, J. H. Wang, and T. A. Springer. 2003. Complex between nidogen and laminin fragments reveals a paradigmatic β-propeller interface. *Nature.* 424:969–974.
4. Kiani, C., L. Chen, Y. J. Wu, A. J. Yee, and B. B. Yang. 2002. Structure and function of aggrecan. *Cell Res.* 12:19–32.
5. Jones, F. S., and P. L. Jones. 2000. The tenascin family of ECM glycoproteins: structure, function, and regulation during embryonic development and tissue remodeling. *Dev. Dyn.* 218:235–259.
6. Aspberg, A., C. Binkert, and E. Ruoslahti. 1995. The versican C-type lectin domain recognizes the adhesion protein tenascin-R. *Proc. Natl. Acad. Sci. USA.* 92:10590–10594.
7. Aspberg, A., R. Miura, S. Bourdoulous, M. Shimonaka, D. Heinegard, M. Schachner, E. Ruoslahti, and Y. Yamaguchi. 1997. The C-type lectin domains of lecticans, a family of aggregating chondroitin sulfate proteoglycans, bind tenascin-R by protein-protein interactions independent of carbohydrate moiety. *Proc. Natl. Acad. Sci. USA.* 94:10116–10121.
8. Oganesyan, V., N. Oganesyan, S. Terzyan, D. F. Qu, Z. Dauter, N. L. Esmon, and C. T. Esmon. 2002. The crystal structure of the endothelial protein C receptor and a bound phospholipid. *J. Biol. Chem.* 277:24851–24854.
9. Ohkubo, Y. Z., and E. Tajkhorshid. 2008. Distinct structural and adhesive roles of Ca^{2+} in membrane binding of blood coagulation factors. *Structure.* 16:72–81.
10. Shikamoto, Y., T. Morita, Z. Fujimoto, and H. Mizuno. 2003. Crystal structure of Mg^{2+} and Ca^{2+}-bound GLA domain of factor IX complexed with binding protein. *J. Biol. Chem.* 278:24090–24094.
11. Meier, M., M. D. Bider, V. N. Malashkevich, M. Spiess, and P. Burkhard. 2000. Crystal structure of the carbohydrate recognition domain of the H1 subunit of the asialoglycoprotein receptor. *J. Mol. Biol.* 300:857–865.
12. Weis, W. I., K. Drickamer, and W. A. Hendrickson. 1992. Structure of a C-type mannose-binding protein complexed with an oligosaccharide. *Nature.* 360:127–134.
13. Besserer, G. M., M. Ottolia, D. A. Nicoll, V. Chaptal, D. Cascio, K. D. Philipson, and J. Abramson. 2007. The second Ca^{2+} binding domain of the Na^{+}-Ca^{2+} exchanger is essential for regulation: crystal

structures and mutational analysis. *Proc. Natl. Acad. Sci. USA*. 47: 18467–18472.

14. Blaustein, M. P., T. H. Charpentier, and D. J. Weber. 2007. Getting a grip on calcium regulation. *Proc. Natl. Acad. Sci. USA*. 47:18349–18350.
15. Chimento, D. P., A. K. Mohanty, R. J. Kadner, and M. C. Wiener. 2003. Substrate-induced transmembrane signaling in the cobalamin transporter BtuB. *Nat. Struct. Biol*. 10:394–401.
16. Herman, P., J. I. B. Vecer, Jr., V. Scognamiglio, M. Staiano, M. de Champdoré, A. Varriale, M. Rossi, and S. D'Auria. 2005. The role of calcium in the conformational dynamics and thermal stability of the D-galactose/D-glucose-binding protein from *Escherichia coli*. *Proteins Struct. Funct. Bioinf.* 61:184–195.
17. Howes, B. D., A. Feis, L. Raimondi, C. Indiani, and G. Smulevich. 2001. The critical role of the proximal calcium ion in the structural properties of horseradish peroxidase. *J. Biol. Chem.* 276:40704–40711.
18. Sotomayor, M., D. P. Corey, and K. Schulten. 2005. In search of the hair-cell gating spring: elastic properties of ankyrin and cadherin repeats. *Structure*. 13:669–682.
19. Sotomayor, M., and K. Schulten. 2008. The allosteric role of the Ca^{2+} switch in adhesion and elasticity of C-cadherin. *Biophys. J*. In press.
20. Phillips, J. C., R. Braun, W. Wang, J. Gumbart, E. Tajkhorshid, E. Villa, C. Chipot, R. D. Skeel, L. Kale, and K. Schulten. 2005. Scalable molecular dynamics with NAMD. *J. Comput. Chem.* 26:1781–1802.
21. MacKerell, A. D., Jr., D. Bashford, M. Bellott, R. L. Dunbrack, Jr., J. Evanseck, M. J. Field, S. Fischer, J. Gao, H. Guo, S. Ha, D. Joseph, L. Kuchnir, K. Kuczera, F. T. K. Lau, C. Mattos, S. Michnick, T. Ngo, D. T. Nguyen, B. Prodhom, I. W. E. Reiher, B. Roux, M. Schlenkrich, J. Smith, R. Stote, J. Straub, M. Watanabe, J. Wiorkiewicz-Kuczera, D. Yin, and M. Karplus. 1998. All-atom empirical potential for molecular modeling and dynamics studies of proteins. *J. Phys. Chem. B*. 102: 3586–3616.
22. Jorgensen, W. L., J. Chandrasekhar, J. D. Madura, R. W. Impey, and M. L. Klein. 1983. Comparison of simple potential functions for simulating liquid water. *J. Chem. Phys*. 79:926–935.
23. Darden, T., D. York, and L. Pedersen. 1993. Particle mesh Ewald. An $N\cdot\log(N)$ method for Ewald sums in large systems. *J. Chem. Phys.* 98:10089–10092.
24. Feller, S. E., Y. H. Zhang, R. W. Pastor, and B. R. Brooks. 1995. Constant pressure molecular dynamics simulation—the Langevin piston method. *J. Chem. Phys*. 103:4613–4621.
25. Martyna, G. J., D. J. Tobias, and M. L. Klein. 1994. Constant pressure molecular dynamics algorithms. *J. Chem. Phys.* 101:4177–4189.